An empirical study on decoupling PNLSS models illustrated on an airplane

Péter Zoltán Csurcsia, Tim De Troyer

Vrije Universiteit Brussel, Department of Engineering Technology
Pleinlaan 2, B-1050 Elsene, Belgium (e-mail: peter.zoltan.csurcsia@vub.ac.be)

Abstract: This paper illustrates a combined nonparametric and parametric system identification framework for modeling nonlinear vibrating structures. First step is the analysis: multiple-input multiple-output measurements are (semi-automatically) preprocessed, and a nonparametric Best Linear Approximation (BLA) method is performed. The outcome of the BLA analysis results in nonparametric frequency response function, noise and nonlinear distortion estimates. Based on this information, a linear parametric (state-space) model is built. This model is used to initialize a high complexity Polynomial Nonlinear State-Space PNLSS model. The nonlinear part of a PNLSS model is manifested as a combination of high-dimensional multivariate polynomials. The last step in the proposed approach is the decoupling: transforming multivariate polynomials into a simplified, alternative basis, thereby dramatically reducing the number of parameters. In this work a novel filtered canonical polyadic decomposition (CPD) is used. The proposed methodology is illustrated on, but of course not limited to, a ground vibration testing measurement of an air fighter.

Keywords: MIMO systems, nonlinearity, data-driven modeling, decoupling, ground vibration testing

1. INTRODUCTION

The goal of this paper is to introduce a simple but efficient state-of-the-art methodology for modeling vibrating structures in real-life experimental situations. The proposed methodology is illustrated on – but not limited to – a ground vibration testing measurement of an aircraft.

Many mechanical and civil structures are inherently nonlinear. The problem lies in the fact that there are many different types of nonlinear systems, that all behave differently. Therefore, modelling is very involved, and universally usable design and modelling tools are not available. As coping with nonlinear systems becomes increasingly important, numerous modeling methods have been proposed. For an overview of the nonlinear modeling techniques we refer to (Kerschen, et al., 2006; Worden & Tomlinson, 2001) and (Schoukens & Ljung, 2019).

In this work multisines are considered as excitation signals. The advantage of the multisines is that 1) there is no problem with spectral leakage/transient,2) they result in high quality frequency response functions (FRFs), and 3) they provide easy-to-understand information about the nonlinearities.

The nonparametric Best Linear Approximation (BLA) framework will be used as a first step (Csurcsia, et al., 2020). The obtained BLA FRF will be then used to initialize a compact linear state-space model. The considered nonlinear model is a polynomial nonlinear state-space (PNLSS) model which consists of the classical linear state-space part (initialized by BLA FRF) and the nonlinear extension. The PNLSS model structure is flexible, as it can capture many different nonlinear dynamic behaviors, however, it suffers from the issue that even for a moderate complexity problem, there are an excessive number of parameters. To overcome this issue, a filtered canonical polyadic decomposition-based decoupling is applied: transforming multivariate polynomials into a simplified representation, thereby dramatically reducing the number of parameters.

The numeric results of the nonparametric (and partly the parametric) work are obtained by the use of the SAMI (Simplified Analysis for Multiple Input Systems) toolbox (Csurcsia, et al., 2020). The initial PNLSS models are obtained by the freely available PNLSS toolbox (Schoukens, 2018). In this work, however, we focus on high level understanding, instead of the usage of the toolbox or elaborating formulas.

This paper is organized as follows. Section 2 briefly describes the considered systems and the main assumptions applied in this work. Section 3 discusses the nonparametric BLA estimation framework. The parametric polynomial nonlinear state-space model is elaborated in Section 4. In Section 5 the description and analysis of the GVT experiments of an aircraft are given. Conclusions can be found in Section 6.

2. BASICS

Several definitions and assumptions must be addressed prior to carrying out any system identification procedure.

2.1 Baseline model

The considered systems are damped, stable, time-invariant, nonlinear mechanical or civil dynamic vibrating structures where the linear response of the system is still present and the output of the underlying system has the same period as the

excitation signal (Csurcsia, 2013)). The dynamics of a linear MIMO system can be nonparametrically characterized in the frequency domain by its Frequency Response Matrix (FRM, (Pintelon & Schoukens, 2012)) G at frequency index *k*, which relates n_i inputs U to n_o outputs Y of *N* measurement samples as follows with sampling frequency of f_s:

$$Y[k] = G[k]U[k] \quad (1)$$

where $G[k] \in \mathbb{C}^{n_o \times n_i}$, $Y[k] \in \mathbb{C}^{n_o \times 1}, U[k] \in \mathbb{C}^{n_i \times 1}$, $k = 0 \dots (N-1)/2$ at frequency $f_k = kf_s/N$.

In order to make the text more accessible, the frequency indices and dimensionalities will be omitted. The system represented by G is linear when the superposition principle is satisfied in steady state.

The output (denoted by Y) is measured with additive, i.i.d. Gaussian noise (denoted by E) such that the measured output $Y_{measured}$ is given by:

$$Y_{measured} = Y + E = GU + E \quad (2)$$

2.2 Multisine excitation

In modern system identification special excitation signals are available to assess the underlying systems in a user-friendly, time efficient way (Schoukens, et al., 2012). In this work flat magnitude multisine signals are used which look like periodic white noise, behave like it but they are not noise. The random phase multisine is a sum of harmonically related sinusoids:

$$u(t) = \sum_{k=1}^{k_{max}} a_k \cos(\omega_1 kt + \varphi_k), \ \varphi_k \sim \mathcal{U}[0,2\pi[\quad (3)$$

where ω_1 is the fundamental angular frequency (that sets the frequency resolution), a_k is the amplitude of the k^{th}harmonic (i.e. frequency index k) set by the user, and k_{max} is the highest harmonic component considered.

If the multisine contains all harmonics, then it is called full (band) multisine. For cases with multiple inputs we recommend using so-called orthogonal random multisines in order to achieve uncorrelated experiments (Csurcsia, et al., 2020).

It is crucial to highlight that it is possible to use multiple periods (blocks) of multisines. Using multiple periods, the SNR of the measurement will be improved. Furthermore, it is highly recommended to enrich the randomness of the (periodic) multisines by adding multiple random realizations. Increasing the number of random realizations results in more robust nonlinearity estimates.

3. BEST LINEAR APPROXIMATION

3.1 Introduction

The Best Linear Approximation (BLA) has been widely used in the last decades to efficiently estimate FRFs (Schoukens, et al., 2012). The BLA of a nonlinear system is an approach of modelling that minimizes the mean square error between the measured output of a nonlinear system and the output of the linear model. In the proposed BLA framework, multiple repeated realizations of the random phase multisine excitation are used. The BLA estimate consists of several components. Fig. 1 shows the structure of the considered BLA estimator.

G_{linear} is the linear phase-coherent component of the model. For the cases, when the output has non-coherent phase behaviour, i.e. when the input phase rotation results in a random phase rotation at the output we can capture the (phase non-coherent) nonlinearities represented by G_s. Increasing the number of random realizations of the multisine signal allows us to tackle the random output phase rotations as an additional (nonlinear) noise source: it does not vary over the repetitions of the same signal segment but only over the different realizations of the signal.

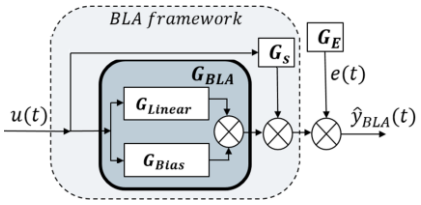

Fig. 1: The theoretical structure of the BLA.

The measurement noise is represented by the component G_E. The usage of periodic excitation reduces the effects of the measurement noise component G_E. The usage of multiple random phase realizations reduces the impact of non-coherent nonlinearities represented by G_s on the BLA estimation.

The (coherent) nonlinearities remaining after multiple realizations of the excitation signal result in a bias error of the BLA, denoted by G_{Bias}. The next section discusses a possibility to reduce the effects of G_S, G_E.

3.2 Multi-dimensional averaging

When the BLA estimation framework is applied, the observed system is excited by random phase multisines. In this work there are *M* different realization of the multisine excitation signal, each realization is repeated *P* period times. The considered model at period p and realization m at frequency bin *k* is given by as an extension of (2) and Fig. 1:

$$\hat{G}^{[m][p]} = Y_{measured}^{[m][p]} U^{[m]^{-1}} = \hat{G}_{BLA} + \hat{G}_S^{[m]} + \hat{G}_E^{[m][p]} \quad (4)$$

where x^{-1} is the generalized (Moore–Penrose) inverse of x.

In order to estimate the BLA FRF in (4), one has to average over *P* periods of repeated excitation signal, and over the *M* different realizations of the excitation signal (see Fig. 2).

A partial FRM estimate $\hat{G}^{[m]}$ is obtained via averaging over the *P* periods. If *P* is sufficiently large, then $\hat{G}_E^{[m]}$ converges to zero (i.e. $\mathbb{E}(\hat{G}_E)$=0). Because the stochastic nonlinear contribution $\hat{G}_S^{[m]}$ does not vary over the repetitions of the same realization, we have to average over the different realizations as well. If M is sufficiently large, then the nonlinear nonlinear noise converges to zero ($\mathbb{E}(\hat{G}_s)$=0).

The estimate of the noise covariance $\hat{\sigma}_{\hat{G}}^2$ of BLA is calculated from the averaged sample variance of each FRM realization. The total variance of the FRM $\hat{\sigma}_{\hat{G}_{BLA}}^2$ is calculated from the sample variance of each different partial BLA estimates $\hat{G}^{[m]}$, see Fig. 2.

The difference between the total variance and the noise variance is an estimate of the variance of the stochastic nonlinear contributions $\hat{\sigma}^2_{NL} \approx \left(\hat{\sigma}^2_{\hat{G}_{BLA}} - \hat{\sigma}^2_{\hat{G}}\right)$. For computational details we refer to (Csurcsia, et al., 2020).

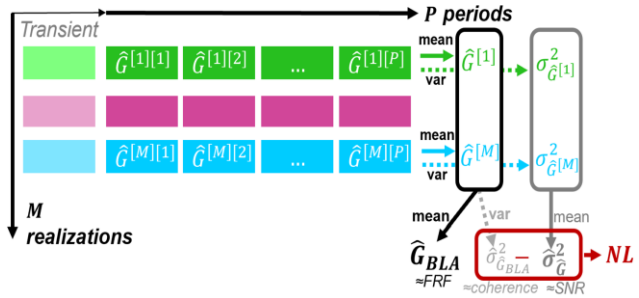

Fig. 2. Evaluation of BLA estimate with 2D averaging.

4. POLYNOMIAL NONLINEAR STATE-SPACE MODEL

A polynomial nonlinear state-space (PNLSS) model consists of the classical linear state-space part and the nonlinear extension part where auto and cross terms of the input and states are considered, see Fig. 3.

It is based on the work of (Paduart, 2008; Decuyper, 2017). It estimates and simulates polynomial PNLSS models from measured data. The PNLSS model structure is flexible, as it can capture many different nonlinear dynamic behaviors (hysteresis, nonlinear feedback, etc.).

The model structure can also easily deal with multiple inputs. The method has already been successfully applied in a large range of applications (mechanical, electronical, electrochemical). Because of the state-space representation it is suitable for control and simulation. The main concern is that the PNLSS is extremely sensitive to unseen input distribution and it might produce unstable simulation output. The foundation of these issues can be seen when looking at the lower level: the kernel of these models is a high-dimensional multivariate polynomial nonlinear function.

A possible solution to this problem is discussed next.

$$\begin{aligned} x(t+1) &= A\,x(t) + B\,u(t) + E\,\zeta(x(t),u(t)) \\ y(t) &= C\,x(t) + D\,u(t) + F\,\eta(x(t),u(t)) \end{aligned}$$

linear state-space model — polynomials in x and u

Fig. 3: The theoretical structure of PNLSS model.

4.1 Decoupling

Decoupling aims at transforming generic multivariate nonlinear functions into decoupled functions. The decoupled structure is characterized by the fact that the relationship is described by a number of univariate functions of intermediate variables. Decoupling is designed to postprocess multivariate nonlinearities which emerge naturally in a large number of dynamical models. The objective is to achieve model reduction while gaining insight into the nonlinear mapping (Decuyper, et al., 2021). Given a generic nonlinear function

$$q = f(p) \tag{5}$$

with $q \in \mathbb{R}^n$ and $p \in \mathbb{R}^m$, the idea is to introduce an appropriate linear transformation of p, denoted V, such that in this alternative basis, univariate functions may be used to describe the nonlinear mapping. The rationale behind the method is that classical regression tools, e.g. a polynomial basis expansion, not necessarily result in a sparse representation. By allowing a rotation towards a more favorable basis, a more efficient representation can be obtained. The decoupled function is then of the following form

$$f(p) = W g(V^T p) \tag{6}$$

where the ith function is $g_i(z_i)$ with $z_i = v_i^T p$, emphasising that all functions are strictly univariate. The number of univariate functions, denoted r, is a user choice which can be used to control the model complexity (r may be larger or smaller than n). It plays a crucial role since it will determine whether the implied equivalence of (6) can be attained. A second linear transformation W maps the function back onto the outputs. The matrices then have the following dimensions: $V \in \mathbb{R}^{m\,x\,r}$ and $W \in \mathbb{R}^{n\,x\,r}$. The decoupled structure is represented graphically in Fig 4.

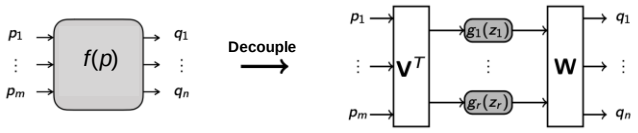

Fig. 4. Illustration of the decoupling technique.

Decoupled functions have a number of attractive features. The fact that the nonlinearity is captured by a set of univariate functions enables to easily visualize the relationship. This may lead to insight. Moreover, decoupled functions are often a much more efficient parameterization of the nonlinearity, resulting in a significant reduction in the number of parameters.

In this work, the filtered CPD approach of (Decuyper, et al., 2021) is used to decouple the multivariate polynomial present in the state equation, $E\zeta(x,u)$ in Fig. 3. The algorithm links the original function to a decoupled function on the basis of its first order derivative information. The method relies on the underlying diagonal structure of the Jacobian, which is a consequence of using univariate functions g_i. Applying the chain rule one obtains the Jacobian of (6)

$$J' = W\mathrm{diag}([h_1(z_1)\ \ldots\ h_r(z_r)])V^T \tag{7}$$

(Dreesen, et al., 2015) found that the underlying diagonality of the Jacobian can be exploited in the decoupling process. It was suggested to construct a third order tensor, $\mathcal{J}$, out of evaluations of the Jacobian of the known function, $f(p)$, and compute a diagonal decomposition, denoted $\mathcal{J}'$, such that $\mathcal{J} \approx \mathcal{J}'$. The tensor decomposition is depicted in Fig. 5. The decomposition returns three matrix factors: both the required linear transformation matrices W and V, together with a third matrix H which stores nonparametric estimates of the first order derivative of the functions g_i.

In (Decuyper, et al., 2021), the decomposition was modified by introducing finite difference filters. This allows for the Jacobian tensor to be decomposed into the more convenient

factors $\{W, V, H'\}$, where H' directly stores evaluations of the univariate functions g_i. The method of (Decuyper, et al., 2021) can be summarized in three steps:

1. Evaluate the Jacobian of the known function, J, in a number of operating points and stack the matrices into a three-way array, i.e. the Jacobian tensor $\mathcal{J} \in \mathbb{R}^{n \times m \times N}$.
2. Factor $\mathcal{J}$ into $\{W, V, H'\}$ by computing a filtered diagonal tensor decomposition (F-CPD).
3. Retrieve the functions, g_i, by parametrizing the nonparametric estimates stored in H'.

The filtered CPD approach is a generic tool which can be used to retrieve decoupled functions, regardless of the function family. Irrespective of the size of the function in terms of *m* and *n*, the decoupling procedure boils down to solving a third order tensor decomposition. Only in a final parameterization step an appropriate basis function is selected for the univariate branches. An additional advantage of the filtered CPD is that the method no longer relies on the uniqueness properties of tensor decomposition. The result is that meaningful decompositions, pointing towards decoupled functions, can be obtained for a user chosen value of *r*, enabling to control the model complexity. For an in-depth discussion on the method the reader is referred to (Decuyper, et al., 2021).

The results illustrate that the nonlinear functions found in PNLSS models may typically be replaced by decoupled functions with a low number of univariate branches. This alludes to the fact that nonliner dynamical systems are in many cases driven by a low number of internal nonlinearties.

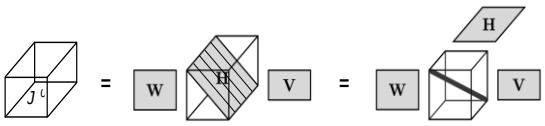

Fig. 5: Centre: a collection of evaluations of the Jacobian of the decoupled function (Eq. (7)), stacked in the third dimension. Left: corresponding third order tensor. Right: extracting the diagonal plane reveals a diagonal tensor decomposition.

5. ILLUSTRATION

5.1 Description of the measurement

This section concerns the ground vibration testing measurement campaign of a decommissioned F-16 aircraft with two dummy payloads mounted at the wing tips, see Fig. 6). The measurement setup consists of 2 shakers–2 force cells (placed under the wings), and various acceleration sensors.

The shaker reference signals are full random phase multisine signals. The sampling frequency is 200 Hz. The period length is 4096 resulting in a frequency resolution of 0.0489 Hz. The smallest excited frequency is 4.541 Hz, the highest excited frequency is 25 Hz.

There are 7 different multisine realizations for each input channel per experiment (in total 14 realizations with the recommended orthogonal phase rotation). Each multisine realization is repeated 3 times.

5.2 Analysis of the measured signals

Before carrying out any analysis of the measurement, we have to ensure that the signals considered are in steady-state, therefore a simple graphical transient check-up is performed: the last period of the first realization – assumed to be in steady-state – is subtracted from every block in that realization, and the blocks with decaying error are discarded. Result: the first transient block has been removed from each realization.

Fig. 6: F-16 ground vibration testing measurement.

In order to make the results more accessible, only the two (low and high) levels of measurements are considered, the input-output signals and FRFs are shown at the driving points only.

The input (force) measurements are shown in Fig. 7. Observe that the excitation signals are almost ideally flat, and the left and right forces are almost identical, however, the noise characteristics are different. For instance, at high level of excitation, the SNR is approximately 50 dB at the right wind, and around 45 dB at the left wing. Furthermore, noise levels move together with the variation of the excitation power (this is an indication of nonlinear behavior because increasing the excitation level results in decreasing SNR).

The output (acceleration) measurements are shown in Fig. 8. Observe that the level-wise noise characteristics are almost identical, but the spectra are different: there is a large difference between the responses at left and right wings. It can also be observed that the resonances have been shifted, which is an indication of nonlinearities.

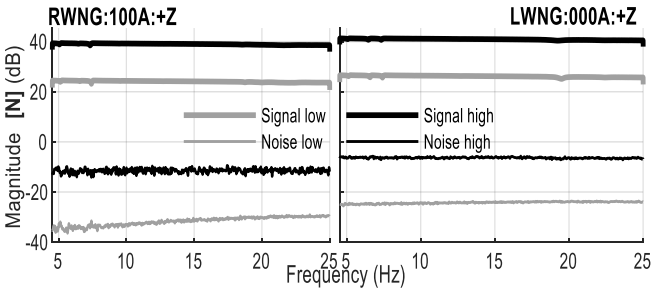

Fig. 7: The input signals and their noise estimates measured at the right and left wings at the low and high amplitude levels.

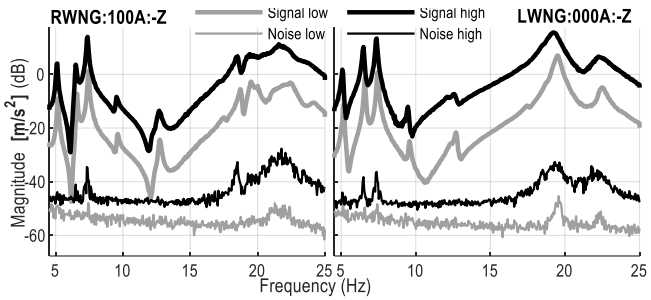

Fig. 8: The output signals and their noise estimates measured at the right and left wings at low and high amplitude levels.

5.3 FRF analysis

Fig. 9 shows the FRFs at the driving points. Despite the fact that the high level excitation is only 15 dB higher than the low level excitation, it can be clearly observed that FRFs at different levels differ a lot from each other, and the estimated nonlinear distortions are larger than the noise estimates.

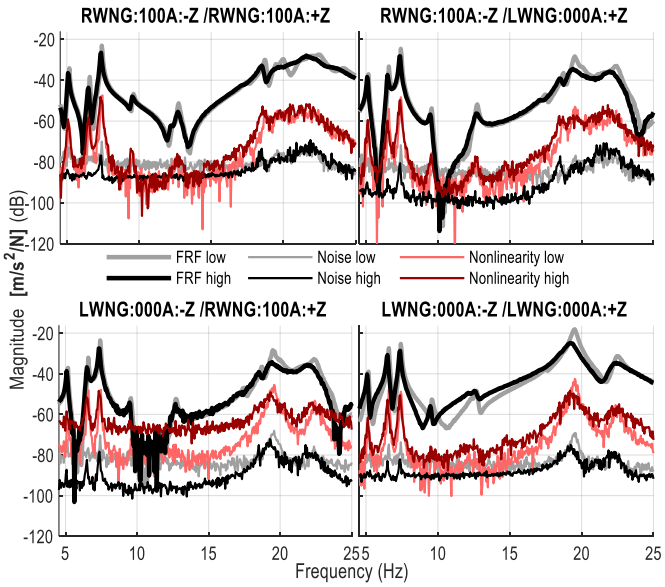

Fig. 9: FRFs, noise and nonlinear distortions estimated at driving points at low and high excitation levels.

5.4 Post-processing

The next step is the parametric post-processing of the data. In order to reduce the computational needs 9 realizations were taken from low and high level. In each realization the periods were averaged (in order to reduce the noise and the computational needs) and the resulting data are split into:

- estimation dataset: 4 realizations (to build a model),
- validation dataset: 4 realizations (to validate a model),
- test dataset: 1 realization (to compare different approaches).

5.5 Parametric BLA

A parametric (state-space) model is built based on low level nonparametric BLA (FRFs and noise) estimates. In order to determine the parametric model order (i.e. number of states), a cross-validated model order scanning method is used between orders 1 and 15 (higher model orders would require considerable memory and computational loads). The best fit (see Fig. 10) w.r.t. cross-validation error was found with a model order of 11, resulting in a total of 169 parameters to be estimated (see **Table 1**).

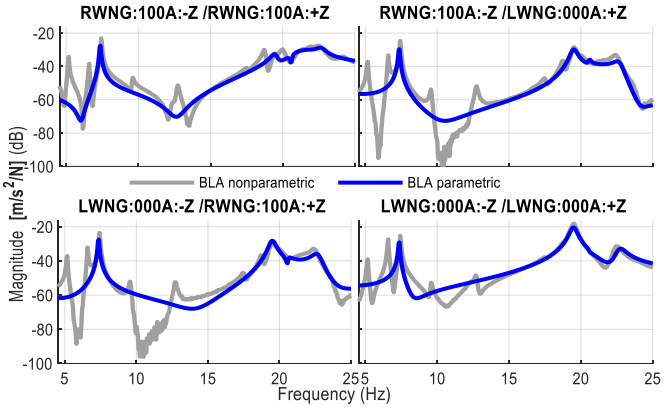

Fig. 10: Parametric and nonparametric FRFs at driving points estimated at the low excitation level.

5.6 PNLSS model

A PNLSS model is initialized with the help of the previously obtained parametric BLA model. In order to reduce the complexity of the problem and the computational needs, only matrix E (state nonlinearities) is considered with 2nd and 3rd order multivariate cross terms resulting in more than 6000 parameters. The PNLSS model is obtained using an optimization routine with 30 iteration steps (Paduart, 2008). The performance of the parametric, nonparametric BLA and PNLSS models is illustrated in Fig. 11 and **Table 1**.

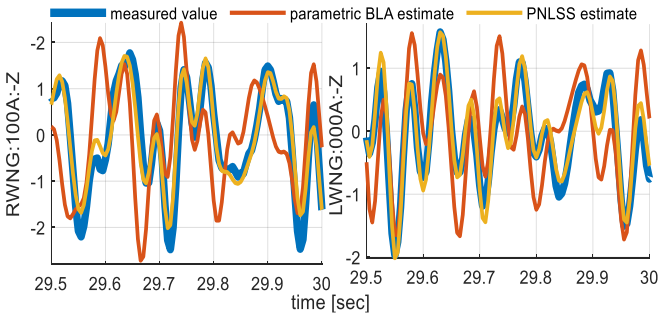

Fig. 11: Fitting illustration on a segment of the test data.

5.7 Decoupling

Applying the F-CPD method to the function the nonlinear part of PNLSS model $E\zeta(x,u)$ dramatically reduces the number of nonlinear parameters from 6006 to 60.

In this paper two cases are considered:

1) decoupling into series of univariate branches based on the full PNLSS model,

2) post-optimization on the decoupled model. The considered number of branches is varied from 1 to 10.

The results illustrated on the relative root mean square (rms) error are shown in Fig. 12. Observe that the further (post) optimization is a high risk-high gain situation: if it is

successful, then the fitting results are excellent, if it is not successful, the modeling errors explode.

The simulation results can be seen in Fig. 13, a numerical comparison can be found in **Table 1**.

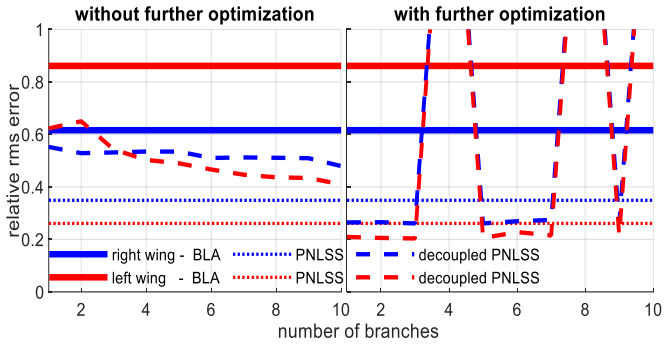

Fig. 12: Fitting results on decoupled PNLSS models compared to parametric BLA and full PNLSS models.

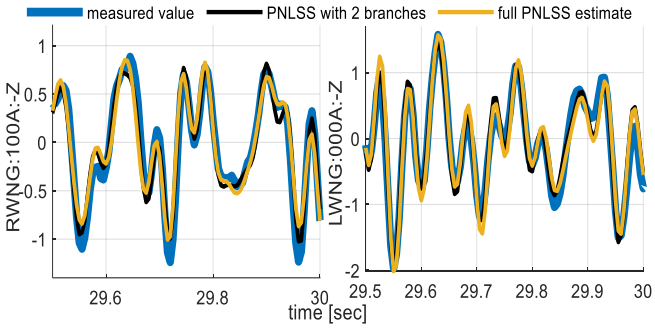

Fig. 13: Fitting illustration on a segment of the test data.

Table 1. Overview of the results

Model	Relative rms error on test data for wing		Number of parameters
	Right	Left	
Nonparametric BLA	1.14	2.126	420
Parametric BLA	0.616	0.861	169
Full PNLSS	0.349	0.261	169+6006
PNLSS with 2 branches	0.528	0.650	169+60
PNLSS with 2 branches - optimized	0.265	0.205	169+60

6. CONCLUSIONS

In this work a novel, semi-automated semi-parametric approach was developed to provide a user-friendly modeling tool for nonlinear MIMO data.

The results turned out to be useful for modelling the nonlinear ground vibration testing of the aircraft because:

- it required minimal user-interaction, and no expert-user was needed
- the input, output and transfer function measurements were nonparametrically characterized
- high-dimensional PNLSS models were successfully decoupled resulting in a very compact powerful model.

ACKNOWLEDGMENTS

This work was funded by the Strategic Research Program SRP60 of the Vrije Universiteit Brussel.

REFERENCES

Csurcsia, P. Z., 2013. Static nonlinearity handling using best linear approximation: An introduction. Pollack Periodica, 8(1).

Csurcsia, P. Z., Peeters, B. & Schoukens, J., 2020. User-friendly nonlinear nonparametric estimation framework for vibro-acoustic industrial measurements with multiple inputs. Mechanical Systems and Signal Processing, Volume 145.

Csurcsia, P. Z., Peeters, B., Schoukens, J. & Troyer, T. D., 2020. Simplified Analysis for Multiple Input Systems: A Toolbox Study Illustrated on F-16 Measurements. Vibration, 3(2), pp. 70-84.

Decuyper, J., 2017. Nonlinear state-space modelling of the kinematics of an oscillating circular cylinder in a fluid flow. Belgium: PhD thesis.

Decuyper, J., Tiels, K. & Schoukens, M. R. a. J., 2021. Retrieving highly structured models starting from black-box nonlinear state-space models using polynomial decoupling. Mechanical Systems and Signal Processing, Volume 146.

Decuyper, J., Tiels, K., Weiland, S. & Schoukens, J., 2021. Decoupling multivariate functions using a non-parametric (Filtered-CPD) approach. Padova, Italy, IFAC Symposium on System Identification.

Dreesen, P., Ishteva, M. & Schoukens, J., 2015. Decoupling multivariate polynomials using first-order information. {SIAM} Journal on Matrix Analysis and Applications, 36(2), pp. 864-879.

Kerschen, G., Worden, K., Vakakis, A. & Golinval, J.-C., 2006. Past, present and future of nonlinear system identification in structural dynamics,. Mechanical Systems and Signal Processing, 20(3), pp. 505-592.

Kolda, T. G. & Bader, B. W., 2009. Tensor decomposition and applications. {SIAM} {R}ev., 51(3), pp. 455-500.

Paduart, J., 2008. Identification of nonlinear systems using Polynomial Nonlinear State Space models. Belgium: PhD thesis.

Pintelon, R. & Schoukens, J., 2012. System Identification: A Frequency Domain Approach. 2nd ed. New Jersey: Wiley-IEEE Press.

Schoukens, J., 2018. Prof. Dr. Johan Schoukens website. http://homepages.vub.ac.be/~jschouk/ [01/01/2020].

Schoukens, J. & Ljung, L., 2019. Nonlinear System Identification: A User-Oriented Road Map. IEEE Control Systems Magazine, 39(6), pp. 28-99.

Schoukens, J., Pintelon, R. & Rolain, Y., 2012. Mastering System Identification in 100 exercises. New Jersey: John Wiley & Sons.

Worden, K. & Tomlinson, G., 2001. Nonlinearity in Structural Dynamics: Detection, Identification and Modelling,. Bristol: Institute of Physics Publishing.